PHYSICAL REVIEW A VOLUME 59, NUMBER 3 MARCH 1999

Long spin relaxation times in a single-beam blue-detuned optical trap

Roee Ozeri, Lev Khaykovich, and Nir Davidson
Department of Physics of Complex Systems, Weizmann Institute of Science, Rehovot 76100, Israel
(Received 5 October 1998)

A scheme to trap atoms in a blue-detuned optical dipole trap, formed with a single laser beam and a holographic phase plate, is demonstrated. 10^5 rubidium atoms are trapped for ($1/e$ lifetime) $\sim$300 msec, at temperatures of $\sim$24 μK and a density of $\sim 7\times 10^{11}$ atoms/cm^3, for a trapping beam detuning of 0.1–30 nm. The time for a trapped atom to scatter one photon off the trapping beam is measured and found to be linear in the trapping laser detuning. At a detuning of 0.5 nm from resonance this time was measured to be $\sim$100 msec, indicating that the atoms are exposed on average only to $\sim$1/700 of the maximal light intensity in the trap. The use of a single laser beam allows for simple dynamical changes of the potential and large adiabatic compressions, while keeping the atoms mainly in the dark. [S1050-2947(99)50903-7]

PACS number(s): 32.80.Pj

Optical dipole traps for laser-cooled atoms [1] offer the possibility for long confinement times and long atomic coherence times, which are important for precision spectroscopy [2], the study of atomic collisions [3] and quantum collective effects [4]. A main limiting mechanism on the atomic coherence is the spontaneous scattering of photons from the trapping laser [2]. This scattering rate can be reduced by an increase in the laser detuning from resonance [5–7]. To further reduce scattering, blue-detuned optical traps, where repulsive light forces confine atoms mostly in the dark, have been developed [2,8,9], achieving atomic coherence times as long as 7 sec [2]. However, all of these schemes for blue-detuned traps are either gravity assisted [9,10] or involve a combination of more then one laser beam [2,8].

In this Rapid Communication we present and demonstrate a scheme to trap atoms in a blue-detuned dipole trap that is not gravity assisted, and that uses a single laser beam detuned 0.1–30 nm above (''blue'') the $5S_{1/2}\rightarrow 5P_{3/2}$ transition in ^{85}Rb. By trapping the atoms in a dark region, where they are least affected by the trapping laser, we combine long storage, heating, and photon-scattering times with extremely strong trap depth, and spring constant of the confining force. Furthermore, the simplicity of the optical arrangement allows simple dynamical changes of the potential.

To produce a light distribution for a blue-detuned trap that is not gravity assisted, a dark volume that is completely surrounded by light is required. To achieve this with a single laser beam, a collimated beam is passed through a circular phase plate that imposes a phase difference of exactly π radians between the central and outer part of the beam and then focused by a lens. Destructive interference between these two parts then ensures a dark region around the focus, which is surrounded by light in all directions.

For a more quantitative analysis we consider a collimated Gaussian beam with $1/e^2$ radius of ω_0 and power P, which passes through a circular π phase plate with radius b and is clipped by a circular aperture with a radius a. The radiuses a and b are chosen such that the integrated amplitude of light is zero, yielding the condition

$$b=\omega_0\sqrt{-\ln\{\tfrac{1}{2}[1+\exp(-a^2/\omega_0^2)]\}}. \qquad (1)$$

When such a light distribution is focused, destructive interference ensures that the center of the focal plane is dark. To determine the intensity distribution around the focal region of the lens we solve numerically the Fresnel diffraction integral. Such a solution is plotted in Fig. 1 for parameters used in our experiment: focal length $f=250$ mm, $\lambda=779$ nm, $\omega_0=6$ mm, and $a=5$ mm. As seen, the dark volume at the focus of the lens is indeed surrounded by light in all directions. The dimensions of the dark volume are similar to those of the bright focal region that would be obtained without the phase plate. Around the dark focal point the light intensity is well approximated by a harmonic potential in the axial direction and a fourth power potential in the radial direction.

To form the circular π phase plates we evaporated a thin dielectric layer (e.g., MgF_2, with a refractive index of $n=1.38$) through a 4-mm diameter radial mask on a glass

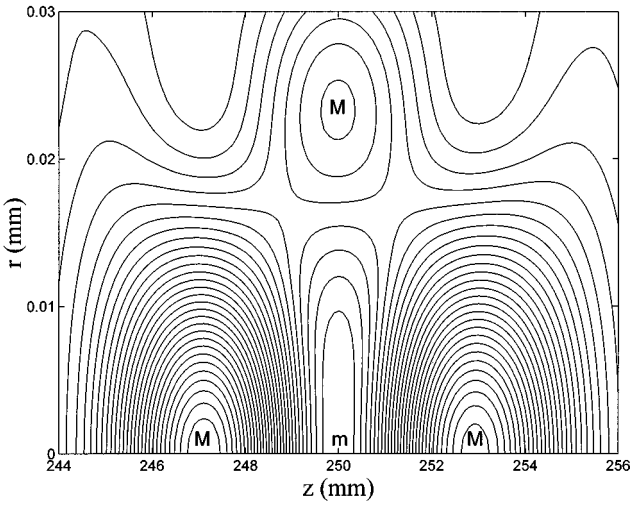

FIG. 1. Contour map for the calculated light intensity distribution $I(z,r)$ around the focus for $w_0=6$ mm, $\lambda=799$ nm, $f=250$ mm, and $a=5$ mm. The dark minimum is labeled m and three bright maxima are labeled M. The distance between the two maxima along the optical axis (trap length) is 5.8 mm, and the distance between the maxima located at the focal plane and the optical axis (trap radius) is 23 μm.

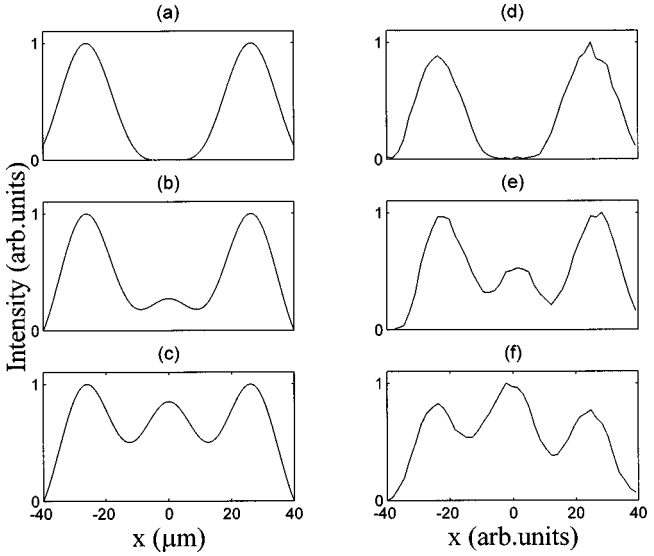

FIG. 2. Cross sections of the trapping beam intensity at different planes along the optical axis, 0, 1, and 1.5 mm from the focal plane. (a)–(c) Calculated. (d)–(f) Measured.

substrate using a commercial optical coating machine. To induce a phase difference of exactly π radians, the thickness of the dielectric coating should be $d=\lambda/[2(n-1)]=676.3$ nm for $\lambda=514.5$ nm (argon laser wavelength). The thickness of the plate was monitored *in situ* during the evaporation process, and was measured afterwards with a α-step profilometer to be 679.5 nm, in good agreement with the required value.

The light intensity distribution around the focal region was measured, using an argon laser and the phase mask described above. Three cross sections of the trap, recorded with a charge-coupled device (CCD) camera at different distances along the optical axis, are shown in Figs. 2(d)–2(f), and compared to the same three cross sections, calculated numerically in Figs. 2(a)–2(c). The good agreement between the measurements and the calculations confirm the accuracy of our optical arrangement. We defined the darkness factor of the trap as the ratio between the light intensity at the center of the trap and the light intensity on the first surrounding ring. *Darkness*=1/750 was measured by scanning a photodiode detector covered with a small pinhole through the image of the focal plane. Finally, similar phase masks were fabricated for a ~780-nm wavelength (for the trap laser), and nearly identical results were obtained. Fortunately, small changes to the laser wavelength (by less than ~100 nm) do not reduce the dankness factor, but merely shift the dark region along the optical axis.

The optical dipole trap was formed with a commercial standing-wave Ti-sapphire laser with an output power of ~1 W, a linewidth of ~40 GHz, and a TEM_{00} (Gaussian) transverse mode. The laser beam was magnified by a telescope into a collimated Gaussian beam with $\omega_0=6$ mm. It was then passed through the π phase plate with an effective radius of 3.5 mm, and through a circular aperture whose diameter was chosen in order to minimize the darkness factor. A minimal darkness factor was achieved in an aperture radius of ~5 mm, in agreement with the calculated value [Eq. (1)] of 5.5 mm. Finally, the beam was focused with a $f=250$-mm lens into the vacuum chamber. The dark focal region was aligned with the center of a magneto-optical trap (MOT), which served as the cold atomic source for the optical trap.

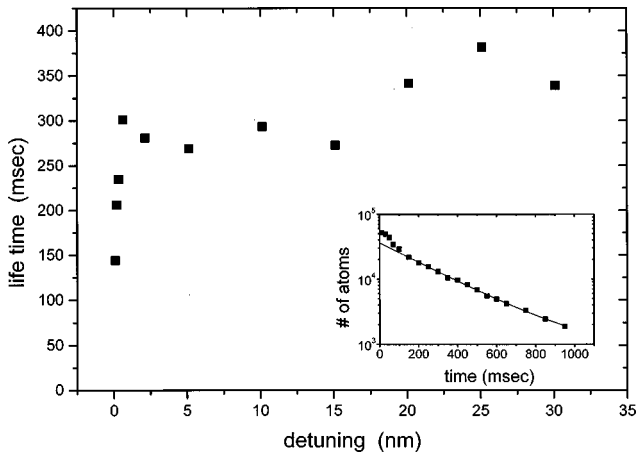

FIG. 3. Trap (1/*e*) lifetime as a function of a trapping beam detuning δ. The inset shows a typical lifetime measurement for $\delta=5$ nm (dots), together with an exponential fit (solid line) that gives the 1/*e* lifetime of 340 msec.

The loading of the optical trap included four stages. First, $\sim 4\times10^8$ ^{85}Rb atoms were loaded, during 500 msec, from the vapor cell (with a pressure of $\sim 3\times10^{-9}$ torr) into a MOT. Second, the intensity of the MOT beams was decreased (to 1.5 mW/cm^2), their detuning was increased (to -30 MHz), and the population fraction in the $F=3$ ground state was reduced to ~0.2, by detuning the repumping laser by -150 MHz from the repumping line. After 30 msec of such ''weak'' and ''temporally dark'' MOT the atomic cloud was compressed to a nearly isotropic Gaussian shape with a peak density of $\sim 5\times10^{10}$ atoms/cm^3. Third, the magnetic field was shut down and the atoms were further cooled to a temperature of 18 μK, as measured by the time-of-flight (TOF) technique. Finally, 3 msec before shutting off the MOT beams, the repumping laser beam was shut off; thus all the atoms in the trap were optically pumped into the $F=2$ hyperfine ground state. During all of the loading stages the trapping beam was on.

A variable time after the MOT beams were shut off the repumping beam was turned on, together with a 1-mm on-resonance probe beam and the induced florescence signal was imaged into a calibrated photomultiplier tube. The number of atoms loaded into the trap was typically measured to be $\sim 10^5$.

The inset of Fig. 3 shows the decay of the number of trapped atoms as a function of the trapping time for a trapping laser detuning of 5 nm. Also shown is an exponential fit for the decay curve for trapping times larger than 100 msec (the excess atoms during the first 100 msec are mainly MOT atoms that have not yet exited the detection volume). We repeated the lifetime measurement for various trapping beam wavelengths and found that they were all fitted well by an exponential decay. The results are shown in Fig. 3. As seen, for trapping laser detuning $\delta>0.5$ nm, the (1/*e*) trap lifetime is nearly independent of δ at around 300 msec. We also verified that for $\delta>0.5$ nm the trap lifetime was inversely proportional to the background pressure in the vacuum chamber. This indicates that the trap lifetime is governed by

collisions with background atoms. For $\delta<0.5$ nm the trap lifetime is approximately proportional to δ. This is consistent with a heating-induced lifetime, since the heating rate is proportional to δ^{-2}, whereas the trap depth is approximately proportional to δ^{-1}. The long lifetime for δ as low as 0.1 nm is only possible for dark traps. Indeed, for a comparable optical trap detuned 0.1 nm red from resonance, we could not find any stable trap at all.

The transverse velocity distribution (or effective temperature) of the trapped atoms was measured, using the TOF technique, 100 msec after their loading. This time was chosen to be much longer than the oscillation period of the trap at any direction and still much shorter than the expected heating time. The spatial distribution of the atomic cloud after a variable time of ballistic expansion was measured by illuminating the atoms for 1 msec by the MOT beams and by imaging the fluorescence on a CCD camera with calibrated magnification. The rms velocity obtained from the fit was 5 cm/sec (or $8.4v_{\mathrm{recoil}}$) for $\delta=1$ nm, and 4 cm/sec (or $6.6v_{\mathrm{recoil}}$) for $\delta=10$ nm. These velocity spreads are similar to those of the MOT atoms that loaded the trap, indicating that the loading did not significantly change the energy of the atoms. A possible error source of our TOF measurements was that the trap shutoff time (~ 100 μsec) was larger than the transverse oscillation period of the trap. Therefore, adiabatic cooling during the shutoff time may have distorted our measurements. We also performed the TOF measurements for the longitudinal dimension of the trap. Here, at the longest ballistic expansion times that still yielded measurable signals, the trap size only increases by $\sim$50%, degrading the expected accuracy of the TOF measurements. We nevertheless measured nearly identical velocity spreads to those of the transverse direction.

To estimate the average density of the atoms in the trap, we had to find the dimensions of the trapped atomic cloud. The cloud length (along the optical axis) was measured directly from the CCD images to be ~ 0.46 mm rms for $\delta=1$ nm. The cloud diameter (in the radial direction) was smaller than the resolution of the imaging system. Therefore, we used the virial relation between the average kinetic energy of atoms in the trap, and the calculated potential distribution to estimate a cloud radius of 4.5 μm rms. This yields a peak atomic density of 6.8×10^{11} atoms/cm^3. The increase in the density as compared to the MOT density can be attributed to the larger spring constant of the optical dipole trap [11].

Next, we investigated the rate in which the trapped atoms spontaneously scatter photons of the trapping laser. This scattering rate determines the heating rate and the atomic decoherence times. For $\delta<0.5$ nm it could already be inferred from the lifetime measurement. For larger detunings, the spontaneous scattering rate was too low to be measured directly. Therefore, we used state-selective detection to monitor the rate of the spontaneous Raman scattering events, which transfer the trapped atoms between the two hyperfine levels of the ground state [12]. By comparing our measurements to the theoretical prediction we are able to estimate the actual light intensity that the trapped atoms are exposed to.

For the measurement the trapped atoms were first prepared in the $5S_{1/2}$, $F=2$ hyperfine level of the ground state by shutting down the repumping laser beam during the last 3 msec of the MOT beams and by keeping it shut for the entire trapping time. After a variable time t, the optical trap was turned off and the probe laser beam, resonant with the $F=3$ level is turned on. The laser-induced fluorescence is proportional to $N_3(t)$, the population of atoms at the $F=3$ level. The total number of atoms at that time $N_3(t)+N_2(t)$ was determined by measuring the fluorescence signal with the repumping laser, resonant with $F=2$, also turned on.

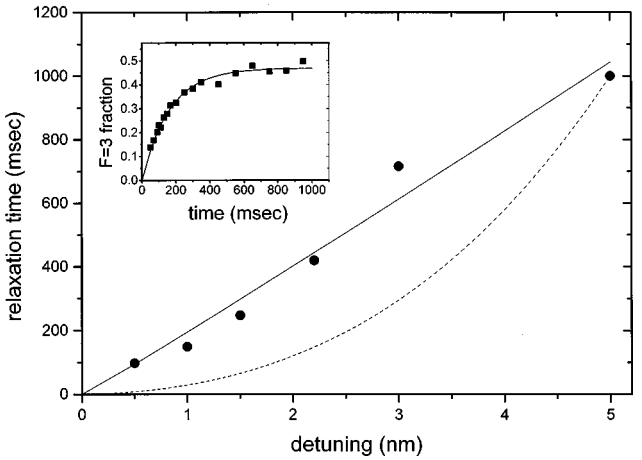

FIG. 4. Measurement of the spin relaxation time τ_{rel} as a function of a trapping laser detuning δ (points) and a power-law fit to the data (solid line), yielding a fit $\tau_{\mathrm{rel}}\sim\delta^{1.04}$. The dashed line shows τ_{rel} calculated for the maximal light intensity in the trap (scaled by a factor of 50). The inset shows a typical measurement of the $F=3$ fraction as a function of time for $\delta=0.5$ nm. The experimental data (points) was fitted to Eq. (2) to yield $\tau_{\mathrm{rel}}=164$ msec.

Typical experimental data for the $F=3$ fraction, for $\delta=0.5$ nm, is shown in the inset of Fig. 4. As seen, the data is well fitted by the function

$$N_3(t)/[N_3(t)+N_2(t)]=c[1-\exp(-t/\tau_{\mathrm{rel}})], \qquad (2)$$

where c is the fraction of atoms having $F=3$ at long times and τ_{rel} is the experimental spin-relaxation time. We repeated the measurements and the fits as a function of δ. The results for τ_{rel} are shown in Fig. 4 for $0.5\ \mathrm{nm}<\delta<5$ nm. Great care was taken to eliminate scattered light in the experiment, which was observed to decrease τ_{rel}. We also verified that the measured τ_{rel} did not depend on the atomic density (such dependence, as well as any other external perturbation, would only decrease τ_{rel}).

We calculated the transition rate $1/\tau_{M,F\rightarrow M',F'}$ between an initial M state in a given hyperfine level F to the state M' in a hyperfine level F' due to the spontaneous scattering of photons from a linearly polarized laser beam, in second-order perturbation theory [13]. In our experiment δ is comparable to the fine structure splitting between excited levels, so the transition amplitudes have to be summed over all possible excited levels in the $5P_{1/2}$ and $5P_{3/2}$ manifolds. The transition rate between an initial F level to a final F' level $1/\tau_{F\rightarrow F'}$ was calculated by averaging over the initial M state rates and summing over the final M' state rates. Finally, a rate equation treatment yields a temporal dependence for the population fraction of the $F=3$ level given by Eq. (2) with a $1/e$ spin-relaxation time given by $1/\tau_{\mathrm{rel}}=1/\tau_{2\rightarrow 3}+1/\tau_{3\rightarrow 2}$. Figure 4 presents the calculated relaxation times (scaled by a

factor of 50) as a function of δ, for laser intensity taken as the maximal laser intensity in the trap.

Several conclusions emerge from Fig. 4. First, the measured spin-relaxation times are much longer than the calculated ones. For example, for $\delta = 0.5$ nm the measured τ_{rel} is 700 times longer than the calculated one. We attribute this increase to the reduction of average laser power that the trapped atoms ''feel'' as compared to the maximal laser power of the trap. The measured atomic ''darkness factor'' is therefore $\sim$1:700 here, in good agreement with our optical measurement.

Another conclusion is seen by comparing calculated and measured functional dependence $\tau_{\mathrm{rel}}(\delta)$. The calculations for a fixed laser power predict that τ_{rel} is proportional to δ^2 for δ much smaller than the fine structure splitting (15 nm for rubidium) and to δ^4 for δ much larger than it [12]. In contrast, the experimental data for $\tau_{\mathrm{rel}}(\delta)$ fits a linear dependence well, as seen in Fig. 4. Such linear dependence indicates that the actual (average) intensity that the atoms feel is inversely proportional to δ, and thus the average dipole potential that they feel is independent of δ. Note that this conclusion, combined with the virial theorem is consistent with our TOF measurements that indicated that the temperature of the trapped atoms is nearly independent of δ. By inverting our theortical calculation and using the virial theorem we can thus use the measured $\tau_{\mathrm{rel}}(\delta)$ to infer the velocity spread of the trapped atoms. For $\delta = 1$ nm, this yields V_{rms} of 3 cm/sec, in good agreement with the TOF measurements of 5 cm/sec.

In summary, we have observed the three-dimensional confinement of atoms in a blue-detuned optical trap, with a trap temperature comparable to that of our MOT and peak density, which is an order of magnitude higher. Long lifetimes were measured even for trapping beam detuning as small as 0.1 nm, where an extremely strong potential of $5 \times 10^4 E_r$ exists. Measured spin-relaxation times reveal a very low spontaneous scattering rate, indicating that the average intensity that the trapped atoms feel is as low as 1/700 of the maximal intensity in the trap (at $\delta = 0.5$ nm). Such large darkness factors also apply to other relaxation processes such as Rayleigh scattering and thus can largely improve atomic coherence times for precise spectroscopic measurements.

The use of a single laser beam simplifies changes to the trap geometry and strength. Replacing the focusing lens in our setup by a zoom lens system with variable f number (F) will enable us to adiabatically change the volume of the trap. A large trap that will mode match the MOT can yield efficient loading, followed by adiabatic compression of the trap to obtain high densities and a runaway evaporative cooling process. The trap volume scales as F^4 and the trap height scales as F^2. Under adiabatic conditions the trap density scales as $F^{3.5}$. The strong confinement will not yield strong energy shifts, since atoms are trapped mainly in the dark. Furthermore, since the optical density in the radial direction is low, optical cooling mechanisms should work in the trap [14]. This trap can also be used as single-beam optical tweezers, to optically trap microscopic metal particles. Finally, more complicated phase plates than the simple circular ones described in this paper can form a large variety of single-beam dark trap potentials with various shapes and sizes.

This work was supported in part by the Minerva Foundation, by the Israel Science Foundation, and by the Israel Ministry of Science. We thank R. Grimm for helpful discussions.

[1] S. Chu, J. E. Bjorkholm, A. Ashkin, and S. Chu, Phys. Rev. Lett. **57**, 314 (1986).
[2] N. Davidson *et al.*, Phys. Rev. Lett. **74**, 1311 (1995).
[3] J. D. Miller, R. A. Cline, and D. J. Heinzen, Phys. Rev. Lett. **71**, 2204 (1993).
[4] D. M. Stamper-Kurn *et al.*, Phys. Rev. Lett. **80**, 2027 (1998).
[5] J. D. Miller, R. A. Cline, and D. J. Heinzen, Phys. Rev. A **47**, R4567 (1993).
[6] C. S. Adams *et al.*, Phys. Rev. Lett. **74**, 3577 (1995).
[7] T. Takekoshi and R. J. Knize, Opt. Lett. **21**, 77 (1996).
[8] T. Kuga *et al.*, Phys. Rev. Lett. **78**, 4713 (1997).
[9] Yu. B. Ovchinnikov, I. Manek, and R. Grimm, Phys. Rev. Lett. **79**, 2225 (1997).
[10] C. G. Aminof *et al.*, Phys. Rev. Lett. **71**, 3083 (1993).
[11] The cloud rms radius was also estimated from its measured length and the calculated potential shape to be 9.3 μm, which is $\sim$2 times larger than the estimate based on the virial theorem.
[12] R. A. Cline, J. D. Miller, M. R. Matthews, and D. J. Heinzen, Opt. Lett. **19**, 207 (1994).
[13] R. Loudon, *The Quantum Theory of Light* (Oxford University Press, Oxford, 1973), Ch. 11.
[14] D. Boiron *et al.*, Phys. Rev. A **57**, R4106 (1998).